inversion against the 2s ground state, and two-photon gain at ω_3 shows up. This gain increases with the probe light intensity, since for degenerate two-photon emission

$$dI_3/dz = B_2 \Delta N I_3^2 \quad (1)$$

holds, where ΔN is the inversion density, and $B_2 I_3^2$ is the two-photon transition rate per atom. At the maximum achievable peak power of the injection pulse, $P_{30} = 3$ kW, the gain in the active zone approximately 2 cm long is $dI_3/I_3 \simeq 20\%$. The full lines represent fits based on the two-photon analog of the Lambert-Beer law,

$$I(z)/I(0) = [1 \pm I(0)/\hat{I}]^{-1}, \quad (2)$$

where $\hat{I}^{-1} = \Delta N \sigma z$, and σ is the emission cross section. However, saturation has been included in the calculation of curves 2 and 3. In contrast, curve 1 is a direct fit of Eq. (2), since saturation is overcome by powerful $3d$-$2p$ superfluorescence following two-photon absorption. This superfluorescence is efficiently quenched upon P_1 pumping which generates appreciable $2p$ population.

The bottom portion of Fig. 3 gives the dependence of the probe gain on the power of the second pump step, P_2. It displays the continuous transition from two-photon absorption to transparency to gain.

In brief, we have demonstrated nondegenerate two-photon light generation and degenerate two-photon amplification in Li vapor. After the (single-photon) laser and maser, the parametric oscillator, and the Raman sources, the two-photon laser is the fourth principally different quantum-optical device. If electric excitation becomes feasible, this novel type of laser will turn out to be particularly useful as a tunable source and as a high-power optical amplifier.

This work was supported by the Deutsche Forschungsgemeinschaft.

[a]On leave from the Institute of Physics, Academia Sinica, Beijing, People's Republic of China.

[1]Maria Goeppert-Mayer, Naturwissenschaften 17, 932 (1929), and Ann. Phys. (Leipzig) 9, 273 (1981).

[2]P. P. Sorokin and N. Braslau, IBM J. Res. Dev. 8, 177 (1964).

[3]A. M. Prokhorov, Science 149, 828 (1965).

[4]R. L. Carman, Phys. Rev. A 12, 1048 (1975).

[5]L. M. Narducci, W. W. Eidson, P. Furcinitti, and D. C. Eteson, Phys. Rev. A 16, 1665 (1977).

[6]S. Barak, M. Rokni, and S. Yatsiv, IEEE J. Quantum Electron. 5, 448 (1969).

[7]S. E. Harris, Appl. Phys. Lett. 31, 498 (1977); L. J. Zych, J. Lukasik, J. F. Young, and S. E. Harris, Phys. Rev. Lett. 40, 1493 (1978).

[8]C. Brechignac and Ph. Cahuzac, J. Phys. B 14, 221 (1981).

[9]D. Cotter and M. A. Yuratich, Opt. Commun. 29, 307 (1979).

[10]Ph. Cahuzac, H. Sontag, and P. E. Toschek, Opt. Commun. 31, 37 (1979).

Energy-Transport, Group, and Signal Velocities near Resonance in Spatially Dispersive Media

Ashok Puri and Joseph L. Birman

Department of Physics, City College, City University of New York, New York, New York 10031

(Received 29 August 1980)

Theoretical results are reported for energy propagation in bounded spatially dispersive (exciton-polariton) media. A remarkable slowing down of the energy-transport velocity V_E is predicted near resonance. For GaAs the decrement is by a factor of 10^4, with $V_E \sim 4\times10^3$ m/sec at resonance. Some comparison is made between energy-transport, group, and signal velocities, and available data.

PACS numbers: 42.10.-s, 78.20.-e

In this Letter we report new theoretical results for the dispersion of the velocity of energy transport, V_E, in a nonlocal or spatially dispersive exciton-polariton medium. Loudon[1] studied energy propagation in an absorbing local dielectric; Bishop and Maradudin[2] extended the analysis to include spatial dispersion, and we follow the latter authors. We find a decrement by a factor of 10^4 in V_E at resonance.

We consider a simplified, idealized situation. The surface of a semi-infinite isotropic spatially dispersive medium lies in the x-y plane, with the medium occupying the half-space $z \geq 0$. A steady-state monochromatic plane electromag-

netic wave is incident normally upon the medium giving rise to two transverse polarized, exciton-polariton plane waves propagating in the medium. These two plane waves are coupled to form the physical polariton, whose velocity of propagation is desired. At the outset, note that each of the constituent plane waves is a coupled photon-exciton and exhibits its own branch dispersion $\omega(k_j)$. This suggests that the group velocity, $V_{Gj}=\partial\omega/\partial k_j$, of each plane wave may be relevant. But in the resonance frequency regime the wave number k_j is a complex quantity for each wave, raising doubt as to the meaning of V_{Gj} defined as a derivative with respect to real part of k_j, $V_{Gj}=d\omega/dk_{jR}$, and in addition the strong coupling between waves raises additional doubt about the significance of V_{Gj}. The signal velocity V_S in spatially dispersive media was introduced and analyzed by Birman and Frankel[3] in order to provide an alternative velocity of propagation, but V_S refers to the first arrival of a substantial laser amplitude, following the decay of precursors, when a square pulse is incident. The velocity of energy transport, V_E, offers another theoretical alternative. We remark that the proofs[4] that energy-transport and group velocities are identical do not apply in the present case since our system is nonlocal, nonhomogeneous (because of the presence of a boundary) and nonconservative as well as having coupled waves. Additional interest in this question arises because of recent experimental reports on slowing down of a wave packet near a resonance. We return to these experiments at the end of this Letter.

Following Ref. 2, we assume a model dielectric function in the medium, of the form (dielectric approximation)

$$\epsilon(\omega,k)=\epsilon_\infty+\frac{4\pi\alpha_0\omega_0^2}{\omega_0^2-\omega^2-i\omega\gamma+Dk^2}, \tag{1}$$

where ϵ_∞ is the background dielectric constant, ω_0 is the resonant frequency, γ is the damping constant, D is $\hbar\omega_0/m^*$, m^* is the exciton mass, and $4\pi\alpha_0$ is the oscillator strength. The physical polariton can be represented as

$$E=\sum_{j=1}^{2}E_j\exp(ik_jz), \tag{2}$$

where k_j is a solution of $(k_j/k_0)^2=\epsilon(k_j,\omega)$, $k_0\equiv\omega/c$, and the E_j are determined from relevant boundary conditions.[5] Notice that $j=1$ and $j=2$ correspond to upper polariton (UP) and lower polariton (LP), respectively.

The energy flux vector $\vec{S}$ in a spatially dispersive medium has been shown by Maddox and Mills,[6] and Bishop and Maradudin,[2] to be the sum of an electromagnetic Poynting vector $\vec{S}_E=(c/4\pi)\vec{E}\times\vec{H}$ and a "mechanical" (in our case excitonic) Poynting vector $\vec{S}_M$, both of which contribute to the energy transport. We now follow Ref. 2 but reinterpret their basic variables $\vec{\xi}$ as $[(m^*)^{1/2}/e_T^*]\vec{p}$ where $\vec{p}$ is the exciton dipole moment and e_T^* the transverse effective charge. The Poynting flux satisfies the equation

$$\nabla\cdot(\vec{S}_E+\vec{S}_M)+\frac{d}{dt}(U_E+U_M)=-\frac{\gamma}{V_a}\dot{\xi}^2-\frac{D}{V_a}\delta(z)\dot{\xi}\cdot\frac{\partial\xi}{\partial z}. \tag{3}$$

Here

$$\vec{S}_E=(c/4\pi)(\vec{E}\times\vec{H}) \tag{4a}$$

$$\vec{S}_M=-(D/V_a)\sum_\beta\hat{x}_\beta\,\theta(z)\,\dot{\vec{\xi}}\cdot\partial\vec{\xi}/\partial x_\beta \tag{4b}$$

$$U_E=(1/8\pi)(\epsilon_\infty E^2+H^2) \tag{4c}$$

$$U_M=V_a^{-1}[\dot{\xi}^2+\omega_0^2\xi^2+D(\nabla\xi)^2]. \tag{4d}$$

V_a is the volume of the unit cell. Using relation (2) and taking the time average one obtains

$$\langle S_E\rangle=(c/8\pi)\,\mathrm{Re}\Big[\Big(\sum_{j=1}^{2}E_je^{ik_jz}\Big)\Big(\sum_{j=1}^{2}E_j^*n_j^*e^{-ik_j^*z}\Big)\Big], \tag{5}$$

$$\langle S_M\rangle=\frac{\omega}{2D}\frac{\epsilon_\infty\Omega_p^2}{4\pi}\,\mathrm{Re}\Big[\Big(\sum_{j=1}^{2}\frac{E_je^{ik_jz}}{(k_j^2-\Gamma^2)}\Big)\Big(\sum_{j=1}^{2}\frac{k_j^*E_j^*e^{-ik_j^*z}}{(k_j^{*2}-\Gamma^{*2})}\Big)\Big], \tag{6}$$

$$\langle U_E\rangle=\frac{1}{16\pi}\,\mathrm{Re}\Big[\epsilon_\infty\Big(\sum_{j=1}^{2}E_je^{ik_jz}\Big)\Big(\sum_{j=1}^{2}E_j^*e^{-ik_j^*z}\Big)+\Big(\sum_{j=1}^{2}n_jE_je^{ik_jz}\Big)\Big(\sum_{j=1}^{2}n_j^*E_j^*e^{-ik_j^*z}\Big)\Big], \tag{7}$$

$$\langle U_M\rangle=\frac{\epsilon_\infty\Omega_p^2}{16\pi D^2}(\omega_0^2+\omega^2+D|\Gamma|^2)\,\mathrm{Re}\Big[\Big(\sum_{j=1}^{2}\frac{E_je^{ik_jz}}{(k_j^2-\Gamma^2)}\Big)\Big(\sum_{j=1}^{2}\frac{E_j^*e^{-ik_jz}}{(k_j^{*2}-\Gamma^{*2})}\Big)\Big], \tag{8}$$

where $n_j = k_j/k_0$ are refractive indices, k_1 and k_2 are wave vectors of propagating modes, Ω_p is a plasma frequency, $\Omega_p{}^2 = 4\pi e_t{}^{*2}/\epsilon_\infty m^* V_a$, and $\Gamma = [-(\omega_0{}^2 - \omega^2 - i\omega\gamma)/D]^{1/2}$.

The energy velocity of the physical polariton is $V_E = \langle S_E + S_M\rangle/\langle U_E + U_M\rangle$, the ratio of magnitude of the flux vector to energy density. In order to proceed, we calculated the magnitudes of the various contributions to V_E using realistic values of the parameters appropriate to the semiconductor GaAs, namely $\hbar\omega_0 = 1.515$ eV, $4\pi\alpha_0 = 0.0013$, $m^* = 0.6\, m_e$, $m_e = 0.5$ MeV, $\epsilon_\infty = 12.55$, $\gamma = 0.1$ cm^{-1}, $\Omega_p{}^2/\omega_0{}^2 = 10^{-3}$, and crystal thickness is 3.7 μm. In the resonance regime of interest ($\omega \sim \omega_0$) we find $\langle S_E\rangle \sim 10^{-1}c$ and $\langle S_M\rangle \sim 10^{-3}c$, or $\langle S_M\rangle \ll \langle S_E\rangle$. It is thus justified to proceed by separating the contribution of upper polariton (UP) branch and lower polariton (LP) branch from $\langle S_E\rangle$ and $\langle S_M\rangle$ in Eqs. (5) and (6). Adding these contributions separately we obtain $\langle S_{UP}\rangle$ and $\langle S_{LP}\rangle$. Likewise $\langle U_{UP}\rangle$ and $\langle U_{LP}\rangle$ are obtained from Eqs. (7) and (8). The contribution of the cross term is thus neglected and we obtain contribution from upper and lower polariton to the Poynting flux, energy density, and energy velocity as

$$\langle S_{UP}\rangle = \frac{c}{8\pi}\,\mathrm{Re}(E_1 E_1{}^* n_1{}^* e^{ik_1 z} e^{-ik_1{}^* z}) + \frac{\omega}{2D}\,\frac{\epsilon_\infty \Omega_p{}^2}{4\pi}\,\mathrm{Re}\left(\frac{E_1 E_1{}^* k_1{}^* e^{ik_1 z} e^{-ik_1{}^* z}}{(k_1{}^2 - \Gamma^2)(k_1{}^{*2} - \Gamma^{*2})}\right), \tag{9}$$

$$\langle U_{UP}\rangle = \frac{1}{16\pi}\,\mathrm{Re}\,[\epsilon_\infty (E_1 E_1{}^* e^{ik_1 z} e^{-ik_1{}^* z}) + E_1 E_1{}^* n_1 n_1{}^* e^{ik_1 z} e^{-ik_1{}^* z}] + \frac{\epsilon_\infty \Omega_p{}^2}{16\pi D^2}\,(\omega^2 + \omega_0{}^2 + D|\,\Gamma\,|^2)\,\mathrm{Re}\left(\frac{E_1 E_1{}^* e^{ik_1 z} e^{-ik_1{}^* z}}{(k_1{}^2 - \Gamma^2)(k_1{}^{*2} - \Gamma^{*2})}\right), \tag{10}$$

$$V_{E\,(UP)} = \langle S_{UP}\rangle/\langle U_{UP}\rangle, \tag{11}$$

$$\langle S_{LP}\rangle = \frac{c}{8\pi}\,\mathrm{Re}\,(E_2 E_2{}^* n_2{}^* e^{ik_2 z} e^{-ik_2{}^* z}) + \frac{\omega}{2D}\,\frac{\epsilon_\infty \Omega_p{}^2}{4\pi}\,\mathrm{Re}\left(\frac{E_2 E_2{}^* k_2{}^* e^{ik_2 z} e^{-ik_2{}^* z}}{(k_2{}^2 - \Gamma^2)(k_2{}^{*2} - \Gamma^{*2})}\right), \tag{12}$$

$$\langle U_{LP}\rangle = \frac{1}{16\pi}\,\mathrm{Re}[\epsilon_\infty (E_2 E_2{}^* e^{ik_2 z} e^{-ik_2{}^* z}) + E_2 E_2{}^* n_2 n_2{}^* e^{ik_2 z} e^{-ik_2{}^* z}] + \frac{\epsilon_\infty \Omega_p{}^2}{16\pi D^2}\,(\omega^2 + \omega_0{}^2 + D|\,\Gamma\,|^2)\,\mathrm{Re}\left(\frac{E_2 E_2{}^* e^{ik_2 z} e^{-ik_2{}^* z}}{(k_2{}^2 - \Gamma^2)(k_2{}^{*2} - \Gamma^{*2})}\right), \tag{13}$$

$$V_{E\,(LP)} = \langle S_{LP}\rangle/\langle U_{LP}\rangle, \tag{14}$$

where $V_{E\,(UP)}$ and $V_{E\,(LP)}$ are upper and lower polariton contributions to the energy velocity.

With use of Eqs. (9)–(14) and the GaAs parameters as given above, the energy velocity was computed, and is shown in the resonance regime as the dotted curves on Fig. 1. Near ω_0, V_E is about 4×10^3 m/sec, a decrement of about 10^4 from nonresonance; this is a remarkable slowing down of energy propagation. We also computed the signal and group velocities [the latter with use of $\partial\omega_j(k)/\partial k_{jR}$, where $k_{jR} = \mathrm{Re}k_j$]. All three velocities are shown in Fig. 1, and in Fig. 2 we exhibit inverse signal velocity, computed following Birman and Frankel,[3] and inverse group velocity computed from the dispersion curves very close to resonance. On the high-frequency side of the resonance $V_{E\,(UP)} \leq V_{G\,(UP)}$. On the low-frequency side, $V_{E\,(LP)} \leq V_{G\,(LP)}$. Exactly at resonance, $V_E \sim 0.1 V_G$. In the resonance region, $V_S < V_G$.

In order to test the theoretical prediction of a sharp decrement in V_E near resonance it would be necessary to prepare a steady-state propagating physical polariton in the indicated geometry. Recently several experimental reports have appeared on a related, but not identical, subject: the slowing down of an optical wave packet with a frequency near resonance in GaAs,[7] CuCl,[8] and CdSe.[9] These experiments have in common that an optical wave packet enters the crystal, and then the arrival of the peak is measured by time-of-flight–type method; they are transient measurements rather than steady state. It is not our purpose here to analyze these experiments in detail but some comparison with our calculations for GaAs is possible. Note that authors of Refs. 7 and 8 compare their data with the calculated group velocity and report agreement, while in Ref. 9 a Fourier-transform method is used. From Fig. 1 here, and the data of Ref. 7, we observe that in GaAs below resonance the peak velocity fits best with the energy-transport velocity; in the resonance regime, V_G, V_S, and V_E are

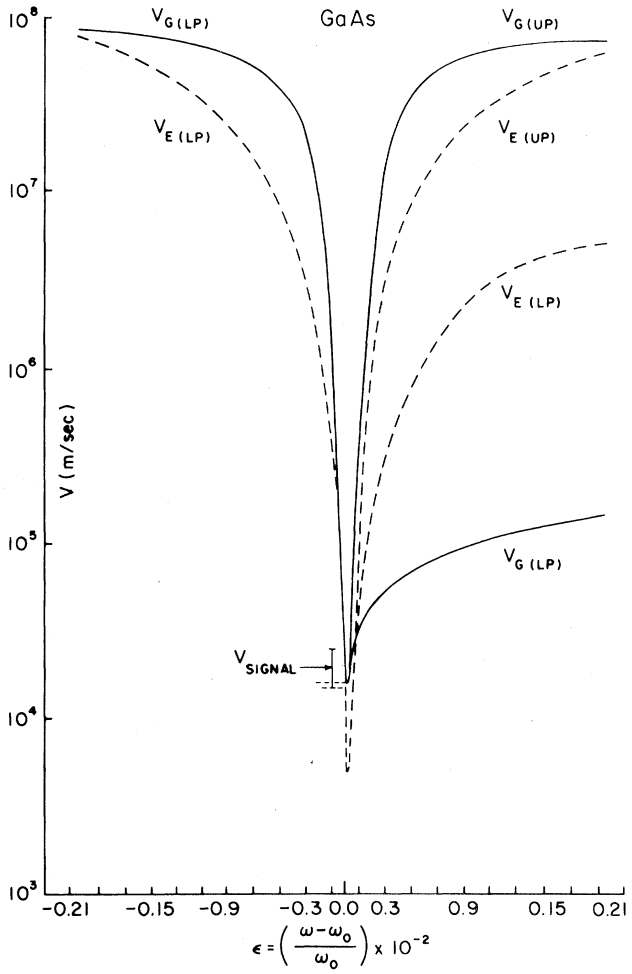

FIG. 1. Energy-transport velocity V_E and group velocity V_G vs reduced frequency ϵ near resonance. Range of signal velocity is shown near resonance. Parameters used are defined in the text.

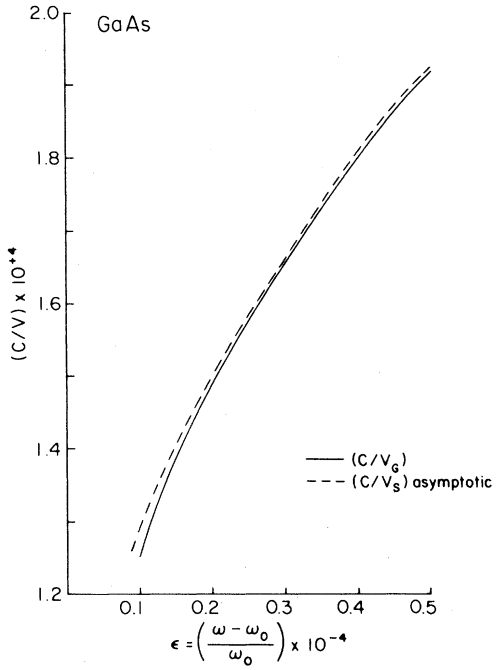

FIG. 2. c times inverse of group and signal velocities vs reduced frequency ϵ in the pseudo-stop-gap region. Parameters used are defined in the text for GaAs.

10, 12, and 15 times smaller than the reported peak velocity; and just above resonance, V_G seems to fit best. At still higher frequencies, effects of higher-lying exciton states, omitted from Eq. (1), need to be included. It was recently pointed out to us by Sturge and Nelson[10] that in these experiments the Gaussian pulse propagation model of Garrett and McCumber[11] may be relevant. We have extended the theory of Ref. 11 to the nonlocal case and find that an incident pulse propagates as a packet composed of several superimposed, distorted Gaussians, and the peak of the resulting packet can in some circumstances travel with an effective velocity close to the "naive" group velocity computed neglecting the imaginary part of the propagation wave number. Our work on this will be reported elsewhere.

We believe it would be of interest to test the predicted slowing down of energy-transport velocity near resonance in excitonic-polariton media by a suitably designed steady-state experiment.

We thank Dr. M. D. Sturge and Dr. D. Nelson for comments. One of us (J. L. B.) acknowledges the receipt of a J. S. Guggenheim Foundation fellowship (1980-1981). This work was supported in part by the U. S. Army Research Office under Grant No. DAAG 29-79-G-0040, the National Science Foundation under Grant No. DMR-78-12399, and Professional Staff Congress-Board of Higher Education Faculty Research Award RF13084.

[1]R. Loudon, J. Phys. A 3, 233 (1970).

[2]M. A. Bishop and A. A. Maradudin, Phys. Rev. B 14, 3384 (1976).

[3]J. L. Birman and M. J. Frankel, Opt. Commun. 13, 303 (1975); M. J. Frankel and J. L. Birman, Phys. Rev. A 15, 2000 (1977).

[4]M. J. Lighthill, J. Inst. Math. Its Appl. 1, 1 (1965), reviews such a proof. The Lagrangian formalism which underlies the proof [see Eq. (82) of this paper] requires local variables, a system without boundaries (otherwise a surface term enters), and a conservative system.

None of these conditions apply in our case.

[5]J. J. Sein, Ph.D. thesis, New York University, 1969 (unpublished), and Opt. Commun. 2, 170 (1970); J. L. Birman and J. J. Sein, Phys. Rev. B 6, 2482 (1972); G. S. Agarwal, D. N. Pattanayak, and E. Wolf, Phys. Rev. Lett. 27, 1022 (1971); A. A. Maradudin and D. L. Mills, Phys. Rev. B 7, 2787 (1973).

[6]R. Maddox and D. L. Mills, Phys. Rev. B 11, 2229 (1975).

[7]R. G. Ulbrich and G. W. Fehrenbach, Phys. Rev. Lett. 43, 963 (1979).

[8]Y. Masumoto, Y. Unuma, Y. Tanaka, S. Shionoya, J. Phys. Soc. Jpn. 47, 1844 (1979).

[9]T. Itoh, P. Lavallard, J. Reydellet, C. Benoît à la Guillaume, to be published.

[10]M. D. Sturge and D. Nelson, private communication.

[11]C. G. B. Garrett and D. E. McCumber, Phys. Rev. A 1, 305 (1970).

Microscopic Derivation of the Helmholtz Force Density

H. M. Lai, W. M. Suen,[a] and K. Young

Department of Physics, The Chinese University of Hong Kong, Shatin, Hong Kong

(Received 30 April 1981)

The Helmholtz force density $\vec{f}^{(H)}$ for a dielectric fluid placed in an electric field is derived microscopically. It is found that in addition to an electrical force, there is also an additional mechanical force proportional to $\vec{E}$ and only the sum of the two equals $\vec{f}^{(H)}$. Time-dependent cases are briefly discussed.

PACS numbers: 41.10.-j, 77.90.+k

Interest in the controversial problem of the force density acting on a dielectric fluid placed in an electromagnetic field[1,2] has recently been revived by laser experiments[3] probing the force density in nonstatic situations. Theoretically, the problem can be approached either macroscopically on the basis of thermodynamic or virtual work principles,[4-6] or microscopically by adding up the forces on individual molecular dipoles.[7-9] Attempts to bridge the two approaches by deriving the thermodynamic result from microscopic models have so far failed: In one derivation, an expression for the effective field, valid at only one point, is differentiated without justification[2]; in another, the electric field is assumed to be parallel to the density inhomogeneity.[10] It has even been alleged that such attempts are doomed to failure.[1]

In this paper we extend the microscopic method, originally formulated for optical frequencies,[7-9] to static situations and find complete agreement with the thermodynamically derived force density of Helmholtz.[4,5,11] The most important point of this paper is the recognition that the force density consists of two distinct components: an electrical part $\vec{f}^{(E)}$ and a mechanical part $\Delta\vec{f}^{(M)}$, with the latter having been neglected in previous treatments.[7-9,12] This separation into two components provides a fresh conceptual understanding of the Helmholtz formula, and predicts different behavior on different time scales.

We begin by recalling the result of Helmholtz, expressible as the following condition for equilibrium[4,5]:

$$\nabla\pi_0(\rho,T) = -\tfrac{1}{2}(\nabla\epsilon)\vec{E}^2 + \tfrac{1}{2}\nabla\left(\rho\frac{\partial\epsilon}{\partial\rho}\vec{E}^2\right) \equiv \vec{f}^{(H)}, \quad (1)$$

where ϵ and ρ are, respectively, the dielectric constant and the number density of the fluid, $\vec{E}$ is the macroscopic field, and π_0 should be taken to be the same pressure function of ρ and the temperature T as in zero field.[4] The right-hand side of (1) is usually called the Helmholtz force density $\vec{f}^{(H)}$. There are, in fact, a number of competing expressions,[13] but (1) seems to agree with experiment,[14] can be reliably derived,[4] and, as we shall see, is also supported by the microscopic calculation.

In attempting to recover (1) microscopically, we first generalize the work of Gordon,[7] Peierls,[8] and others[9] to arbitrary static fields acting on a possibly inhomogeneous medium. The medium is assumed to be nonpolar, nonmagnetic, isotropic, and described by the Clausius-Mossotti relation; moreover, only effects up to order $\vec{E}^2$ will be considered. The brief and physically intuitive derivation given here can be made rigorous by starting from an exact kinetic equation.[15]

The electrical force acting on a dipole $\vec{\mu}$ is

